*Geological Survey of Japan Cruise Report No. 20, p. 227-241, 1984*

# XIV. MINERALOGY AND INTERNAL STRUCTURE OF MANGANESE NODULES OF THE GH80-5 AREA

*Akira Usui*

## Introduction

Mineral composition and internal structure of manganese nodules are most important in determining their physical and chemical characteristics. Earlier investigations have shown that surface features (rough to smooth) of nodules are almost exclusively correlated to constituent minerals, and that similar features corresponding to rough and smooth surfaces are also present inside nodules (USUI, 1979). Therefore precise mineralogical description gives us more detailed external and internal characteristics of nodules than simple morphological description.

In order to confirm the relationships of mineral composition to external and internal morphology and chemical composition, powdered samples were prepared from defined portions of each nodule. Comparative studies were made on the same samples by means of X-ray powder diffraction method, microscopy and chemical analyses.

Internal structure of the samples are described on the basis of megascopic and microscopic observations on polished sections taking the X-ray diffraction data into account. One or more nodule samples were selected from each station mainly along detailed survey lines (USUI, Chapter IX in this cruise report).

## Determination of mineral constituents

Mineralogy of marine manganese minerals has been controversial because of their low crystallinity and small crystal size. Terminological problems contended by many workers are summarized by BURNS and BURNS (1977, 1979). Table XIV-1 lists reported mineral terms of marine manganese nodules. I adopt following terms in this article; 10 Å manganate, 7 Å manganate, and δ-$MnO_2$. The terms δ-$MnO_2$ is restricted to the 2 diffraction line type.

These mineral constituents can be determined by X-ray diffraction method and reflecting microscope independently. The X-ray diffraction method gives semi-

Table XIV-1 Comparison of mineral terms for marine manganese nodules

| | | | |
|---|---|---|---|
| 10 Å manganite | 7 Å manganite | δ-$MnO_2$ | Buser and Grütter (1956) |
| todorokite | birnessite | δ-$MnO_2$ | Burns and Burns (1977) |
| buserite | birnessite | δ-$MnO_2$ (random-stacked or tubostratic) | Giovanoli and Burki (1975) |
| todorokite | birnessite | vernadite | Chukhrov et al. (1979) |
| 10 Å manganate | 7 Å manganate | δ-$MnO_2$ (Z-disordered) | Arrhenius et al (1979) |
| 10 Å manganate | 7 Å manganate | δ-$MnO_2$ | This study |

Table XIV-2 Criteria for optical determination of nodule minerals under reflecting microscope (Usui, 1979)

| | 10 Å manganate phase | $\delta$-$MnO_2$ phase |
|---|---|---|
| Color | light grey | dark grey |
| Reflectivity (wave length 460 nm) | high (ca. 13%) | low (ca. 8%) |
| Anisotropism | strong | none |
| Hardness (Vicker's hardness number) | high (55-112, mean 82) | low (10-24, mean 17) |
| Internal reflection | none | none |

quantitative mineral contents in nodules while the microscopy precise microstructure of the mineral constituents in each nodule sample.

X-ray powder diffraction analyses were accomplished in the constant measurement conditions using the diffractometer Type RAD-rA (Rigaku Denki Co. Ltd.) with a monochromator. Powder samples mounted in standard glass holders were subjected to nickel-filtered $CuK_\alpha$ radiation at 40 kV and 160 mA during 8° (2 $\theta$)/min scan from 3° to 45° (2 $\theta$). Manganese minerals were identified on diffractograms according to six characteristic peaks at 10, 7, 5, 3.5, 2.4 and 1.4 Å d-spacings. 10 and 5 Å reflections are diagnostic of 10 Å manganate, while 2.4 Å reflections is responsible to both 10 Å manganate and $\delta$-$MnO_2$. Amounts of 10 Å manganate are estimated from the peak height at 10 Å. Amounts of $\delta$-$MnO_2$ are estimated from the peak heights at 10 and 2.4 Å assuming that the intensity ratio at 10 and 2.4 Å reflections of 10 Å manganate is 5.0. Analytical error of the amounts is in the order of 10%. Accessory silicate minerals, such as quartz, feldspars, clay minerals and zeolites, are examined on the basis of ASTM data files.

Microscopic identification of manganese minerals is based on earlier works. Two principal manganese phases, the 10 Å manganate and $\delta$-$MnO_2$, are distinguishable on reflecting microscope according to reflectivity and anisotropism, except for submicroscopic lamination of both phases. Silicate minerals are hard to identify under reflecting microscope. The criteria for microscopic identification of manganese minerals are listed in Table XIV-2.

**X-ray diffraction analysis**

The X-ray diffraction study has shown that dominant manganese minerals of these nodules are 10 Å manganate and 2 line form $\delta$-$MnO_2$ but distinct 7 Å reflections responsible to manganese minerals are not found, which is consistent with our earlier work (Usui, 1982). Other manganese-free minerals in manganese nodules determined are quartz, plagioclase, and montmorillonite. The results of X-ray diffraction analyses are listed in Table XIV-3. The analysis numbers in the table are comparable to those for chemical analyses in Table XV-1.

To examine the relationship between surface structure and mineral composition, powder samples were taken from defined portions of nodules. The types of surface feature described for GH80-5 nodules, s, s·r, r, are variably developed on nodule tops, bottoms, and entire surfaces (Usui, Chapter IX in this cruise report). The results of these X-ray diffraction analyses reveal that the surface feature is exclusively correspondent to either of the two constituent minerals. Smooth surface (s) is always

Table XIV-3 Relative mineral composition of manganese nodules

**Area I**

| Line | AN* | St./Sample No | Nodule sample | | | Mineral abundance | | | | | |
|---|---|---|---|---|---|---|---|---|---|---|---|
| | | | Shape | Surface | Part | TM | DM | Qtz | Ph | Pc | Mmt |
| | 1 | 1979 FG252-1 | IS | 1 | O (1-3) | tr | ×× | × | — | — | — |
| | 2 | | | | I | tr | ×× | × | ×× | — | — |
| | 3 | 1983 FG256-1 | D | 3 | W | × | × | ×× | × | tr | — |
| | 4 | FG256-2 | D | 3 | T (0-2) | × | ×× | ×× | — | — | — |
| | 5 | | | | B (0-1) | ××× | tr | ×× | — | — | tr |
| | 6 | 1984 B34 | S | 6 | W (0-7) | ×× | — | ××× | tr | — | × |
| | 7 | FG257 | S | 6 | W (0-7) | ××× | — | ×× | ×× | — | — |
| | 8 | 1985 FG258-1 | S | 6 | W (0-10) | ×× | tr | ×× | × | — | tr |
| | 9 | 1988 FG261-1 | S | 1 | O (0-3) | tr | × | × | — | — | — |
| | 10 | | | | I | — | ×× | × | ×× | × | — |
| | 11 | FG261-2 | D | 1 | W | tr | ×× | × | × | — | — |
| | 12 | 1989 B36 | D | 1 | W | tr | ×× | ×× | — | — | — |
| | 13 | 1990 FG236-1 | D | 1 | W | × | ×× | × | tr | — | — |
| | 14 | 1991 B37 | DP | 1 | W | tr | ×× | × | × | — | — |
| I-a | 15 | 1987 B35 | S | 6 | W (0-10) | ×× | — | × | — | — | — |
| | 16 | FG260 | S | 6 | W (0-10) | ×× | × | ×× | × | tr | tr |
| | 17 | 1992 FG267 | S | 6 | W (0-10) | ××× | tr | ××× | × | — | — |
| | 18 | 1993 FG268 | S | 6 | W (0-10) | ××× | — | ××× | tr | — | — |
| | 19 | 1994 B38 | S | 6 | W (0-10) | ×× | × | ××× | tr | — | — |
| | 20 | 1995 FG269 | S | 6 | W (0-10) | ××× | × | ×× | — | tr | — |
| | 21 | 1996 FG270 | ISP | 3 | T (0-1) | × | × | ×× | ×× | — | tr |
| | 22 | | | | B (0-2) | × | × | ×× | ×× | — | tr |
| | 23 | 1997 FG271 | S | 6 | W (0-10) | ×× | × | ××× | tr | — | — |
| | 24 | 1998 B39 | S | 4 | W | ×× | tr | ×× | × | — | — |
| | 25 | | D | 4 | W | ×× | × | ×× | tr | — | — |
| | 26 | 1999 FG272 | IS | 2 | T (0-2) | × | × | ×× | — | — | — |
| | 27 | | | | I | tr | ×× | × | ×× | — | — |
| | 28 | | | | B (0-1) | × | × | ×× | — | — | — |
| | 29 | 1986 P196 | ID | 2 | T (0-2) | × | × | ×× | — | — | — |
| | 30 | FG259-1 | IDP | 2 | T (0-2) | tr | × | × | tr | — | — |
| | 31 | | | | I | tr | ×× | × | ×× | — | tr |
| | 32 | | | | B (0-2) | ×× | × | ×× | tr | — | tr |
| I-b | 33 | 1982 FG255-2 | D | 2 | T (0-2) | ×× | × | × | — | — | — |
| | 34 | | | | I | — | ×× | × | tr | — | — |
| | 35 | 2000 FG273 | DP | 1 | T (0-2) | tr | ×× | × | — | — | — |
| | 36 | | | | I | — | ×× | × | tr | — | — |
| | 37 | 2001 FG274 | ID | 1 | O (0-2) | × | × | ×× | — | — | — |
| | 38 | | | | I | × | ×× | × | tr | — | tr |
| | 39 | 2002 FG275 | ISP | 1 | O (0-3) | tr | × | ×× | — | — | — |
| | 40 | | | | I | tr | ×× | × | tr | × | tr |
| | 41 | 2003 B40 | ISP | 3 | T (0-2) | × | × | ×× | — | — | — |
| | 42 | | | | I | — | ×× | × | × | — | — |
| | 43 | | | | B (0-1) | ××× | — | ×× | — | — | — |
| | 44 | 2004 FG276 | SP | 3 | T (0-2) | × | × | ×× | — | — | — |
| | 45 | | | | I | ×× | × | ×× | ×× | — | — |
| | 46 | | | | B (0-1) | × | × | ×× | — | — | — |
| | 47 | 2005 FG277 | S | 6 | W (0-5) | ×× | — | ××× | × | — | — |
| | 48 | | D | 6 | O (0-2) | ×× | × | ×× | tr | — | — |

* : analysis number.

Table XIV-3 (continued)

| Line | AN | St./Sample No. | | Nodule sample | | | Mineral abundance | | | | | |
|---|---|---|---|---|---|---|---|---|---|---|---|---|
| | | | | Shape | Surface | Part | TM | DM | Qtz | Ph | Pc | Mmt |
| | 49 | | | | | I (2-10) | × | ×× | ××× | ×× | ×× | tr |
| | 50 | 2006 | P199 | S | 6 | W | ××× | — | ××× | ×× | tr | — |
| | 51 | 2007 | FG278 | S | 6 | O (0-10) | ××× | — | ×× | tr | tr | — |
| | 52 | | | | | I | ×× | × | ×× | ×× | tr | — |
| | 53 | 1981 | B33 | S | 6 | O (0-15) | ××× | — | ×× | tr | — | tr |
| | 54 | | | | | I | ×× | tr | ×× | ×× | — | — |
| | 55 | | FG254 | S | 6 | W (0-10) | ××× | — | ×× | — | — | — |
| | 56 | 2008 | FG279 | S | 6 | W (0-15) | ×× | × | ×× | ×× | × | — |
| | 57 | 2009 | FG280 | D | 6 | W (0-20) | ××× | — | ×× | tr | — | — |
| | 58 | 2010 | FG281 | S | 6 | W (0-5) | ××× | — | ×× | tr | — | — |
| | 59 | | | D | 6 | W (0-20) | ××× | — | ×× | tr | — | — |
| | 60 | 2011A | FG285 | D | 4 | O (0-2) | ×× | × | ×× | — | — | tr |
| | 61 | | | | | I | ×× | — | × | tr | — | — |
| | 62 | 2012 | FG282 | S | 6 | W (0-4) | ××× | — | ××× | — | — | — |
| | 63 | 2013 | FG283 | S | 6 | W (0-10) | ××× | — | ×× | — | — | — |
| | 64 | | | 6 | | W (0-20) | ×× | tr | ×× | tr | — | — |
| | 65 | 2014 | B41 | D | 5 | O (0-1) | ××× | — | ×× | — | — | × |
| | 66 | | | | | I | × | × | ×× | ×× | × | tr |
| | 67 | 2015 | FG284 | IDP | 2 | O (0-2) | × | × | ×× | — | — | — |
| | 68 | | | | | I | × | × | ×× | ×× | × | — |
| | 69 | 1980 | FG253-1 | IDP | 3 | T (0-2) | tr | × | × | — | — | — |
| | 70 | | | | | I | × | × | × | ×× | — | — |
| | 71 | | | | | B (0-1) | ××× | — | × | — | — | — |

Area II

| Line | AN | St./Sample No. | | Nodule sample | | | Mineral abundance | | | | | |
|---|---|---|---|---|---|---|---|---|---|---|---|---|
| | | | | Shape | Surface | Part | TM | DM | Qtz | Ph | Pc | Mmt |
| | 72 | 2019 | B43 | S | 6 | W | ××× | — | ××× | tr | — | — |
| | 73 | 2020 | B44 | D | 6 | W | ××× | — | ××× | tr | — | — |
| | 74 | | FG289 | D | 6 | O (0-3) | ××× | — | ××× | tr | tr | — |
| | 75 | | | | | I (3-8) | — | ×× | ××× | ×× | ×× | ×× |
| | 76 | 2023 | EG292 | I | 6 | W | ×× | × | ×× | — | × | × |
| | 77 | 2022 | FG293 | ID | 6 | O (0-2) | ××× | — | ××× | tr | — | — |
| | 78 | | | | | I | tr | ×× | ×× | tr | — | — |
| | 79 | 2025 | FG294 | I | 6 | W | ×× | × | ××× | tr | — | — |
| | 80 | 2028 | FG297-2 | IS | 1 | O (0-2) | × | × | ×× | — | — | — |
| | 81 | | | | | I | — | ×× | × | — | × | × |
| II-a | 82 | 2021 | FG290-1 | D | 6 | W | ××× | — | ××× | tr | tr | — |
| | 83 | | FG290-2 | S | 6 | W | ××× | — | ××× | — | — | — |
| | 84 | 2041 | FG304 | SP | 6 | O (0-2) | ×× | — | ××× | tr | — | — |
| | 85 | | | | | I | × | × | ×× | ×× | — | — |
| | 86 | 2042 | B55 | S | 6 | W | ××× | tr | ×× | — | — | — |
| | 87 | 2043 | FG305 | D | 6 | W | ×× | tr | ×× | tr | tr | tr |
| | 88 | 2044 | B56 | ID | 5 | O (0-1) | ×× | tr | ×× | — | — | — |
| | 89 | | | | | I | tr | ×× | ×× | ×× | × | tr |
| | 90 | 2046 | FG307 | IDP | 5 | T (0-2) | × | ×× | ×× | tr | — | — |
| | 91 | | | | | I | × | ×× | ×× | ×× | — | tr |
| | 92 | | | | | B (0-1) | ××× | tr | ×× | — | — | — |

Table XIV-3 (continued)

| Line | AN | St./Sample No. | | Nodule sample | | | Mineral abundance | | | | | |
|---|---|---|---|---|---|---|---|---|---|---|---|---|
| | | | Shape | Surface | Part | TM | DM | Qtz | Ph | Pc | Mmt |
| | 93 | P206 | ID | 4 | O (0-3) | × | ×× | × | — | — | — |
| | 94 | | | | I | tr | ×× | ×× | ×× | tr | — |
| | 95 | 2045 | FG306 | IS | 2 | T (0-1) | × | × | ×× | — | — | — |
| | 96 | | | | | I | tr | ×× | × | × | tr | tr |
| | 97 | | | | | B (0-1) | ×× | × | × | — | — | — |
| | 98 | 2022 | B45 | ID | 2 | T (0-3) | tr | ×× | ×× | — | — | — |
| | 99 | | | | | I | × | ×× | × | × | tr | — |
| | 100 | | | | | B (0-1) | ×× | × | × | — | — | — |
| | 101 | | FG291 | ID | 2 | O (0-2) | × | × | × | — | — | — |
| | 102 | | | | | I | — | ×× | × | tr | tr | — |
| II-b | 103 | 2026 | FG295-2 | D | 6 | O (0-2) | ×× | tr | ×× | — | — | — |
| | 104 | | | | | I | × | × | ×× | ×× | tr | tr |
| | 105 | | FG295-1 | S | 6 | O (0-2) | ×× | tr | ×× | × | — | — |
| | 106 | | | | | I (2-10) | × | × | × | ×× | — | tr |
| | 107 | 2034 | B51 | D | 6 | O (0-1) | ××× | — | ×× | — | — | — |
| | 108 | | | | | I | ×× | tr | ×× | tr | tr | — |
| | 109 | 2033 | FG300 | S | 6 | O (0-10) | ××× | — | ××× | — | — | — |
| | 110 | | | | | X (10-20) | ××× | — | ××× | tr | — | — |
| | 111 | | | | | I (20-40) | × | ×× | ×× | tr | × | — |
| | 112 | 2032 | B50 | SP | 6 | O (0-1) | ××× | × | ×× | — | — | — |
| | 113 | | | | | X (1-10) | ×× | tr | ×× | tr | — | — |
| | 114 | | | | | I (10-40) | — | ×× | ×× | tr | — | — |
| | 115 | 2031 | FG299 | IS | 2 | O (0-3) | ×× | tr | ×× | — | — | — |
| | 116 | | | | | I | — | ×× | ×× | × | × | tr |
| | 117 | 2030 | B49 | ID | 2 | B (0-1) | ××× | — | ×× | — | — | tr |
| | 118 | | | | | T | × | ×× | ××× | — | — | — |
| | 119 | | | | | I | tr | ×× | × | — | — | — |
| | 120 | 2029 | FG298 | ID | 2 | T (0-2) | × | ×× | ×× | — | — | — |
| | 121 | | | | | I | — | ×× | × | — | — | — |
| | 122 | | | | | B (0-1) | × | × | ×× | — | — | — |
| | 123 | 2027 | FG296 | ID | 4 | O (0-1) | ×× | × | ×× | tr | tr | — |
| | 124 | | | | | I | — | ×× | tr | — | — | — |
| | 125 | | | C | 1 | W (0-5) | — | ×× | tr | — | — | — |
| | 126 | | B48 | IDP | 1 | O (0-2) | × | × | ×× | — | — | — |
| | 127 | | | | | I | — | ×× | × | × | tr | — |
| II-c | 128 | 2018 | FG287-2 | S | 6 | W (0-10) | ××× | — | ×× | — | — | — |
| | 129 | | FG287-1 | SP | 6 | W | ××× | — | ××× | — | — | — |
| | 130 | 2040 | B54 | S | 6 | W | ××× | — | ××× | tr | — | tr |
| | 131 | 2039 | FG303 | S | 6 | W (0-7) | ××× | — | ××× | — | — | — |
| | 132 | 2038 | B53 | S | 6 | W (0-7) | ××× | — | ××× | — | — | — |
| | 133 | 2037 | FG302 | S | 6 | W (0-12) | ××× | — | ××× | tr | — | — |
| | 134 | 2036 | B52 | IS | 6 | O (0-1) | ××× | — | ×× | — | — | × |
| | 135 | | | | | X (1-5) | × | × | × | — | — | — |
| | 136 | | | | | X (5-15) | tr | × | × | tr | — | — |
| | 137 | | | | | I (15-30) | — | ×× | × | — | tr | — |
| | 138 | 2035 | FG301 | ID | 4 | O (0-3) | ×× | tr | ×× | — | — | — |
| | 139 | | | | | I | tr | ×× | × | tr | — | — |
| | 140 | 2017 | FG286 | ID | 3 | T (0-4) | × | ×× | ×× | tr | — | — |
| | 141 | | | | | I | — | ×× | ×× | — | × | — |

Table XIV-3 (continued)

| Line | AN | St./Sample No. | Nodule sample | | | Mineral abundance | | | | | |
|---|---|---|---|---|---|---|---|---|---|---|---|
| | | | Shape | Surface | Part | TM | DM | Qtz | Ph | Pc | Mmt |
| | 142 | | | | B (0-1) | ×××| × | ××× | — | — | — |
| | 143 | B42 | ID | 3 | T (0-3) | × | ×× | × | — | — | — |
| | 144 | | | | I | — | ×× | × | tr | tr | — |
| | 145 | | | | B (0-1) | ××× | × | ×× | — | — | tr |

1) Nodule shape S: spherical, D: discoidal, I: irregular, P: polynucleate, C: crust.
2) Nodule surface 1: s, 2: s+s·r, 3: s+r, 4: s·r, 5: s·r+r, 6: r.
3) Analyzed part W: whole, O: outermost, I: innermost, T: top, B: bottom, X: others. Depth from surface (in mm) is in parenthesis.
4) Minerals TM: 10Å manganate, DM: 2 line form $\delta$-$MnO_2$ (calculated), Qtz: quartz, Ph: phillipsite, Pc: plagioclase, Mmt: montmorillonite.
5) Abundance ××× : abundant, ×× : common, × : present, tr: traceable, — : not detected.

composed of the $\delta$–$MnO_2$ phase while rough surfaces (r) and intermediate surfaces (s·r) are always composed of 10 Å manganate. However, thickness of the layer of each mineral constituent on nodule surface is variable. Interminate surface feature (s·r) consists of very thinly developed rough structure of the 10 Å manganate on smooth structure of the $\delta$–$MnO_2$ phase. The chemical compositions of each powder sample are also remarkably consistent with mineral composition (USUI, Chapter XV in this cruise report).

Silicate minerals are incorporated in nodules as fine particles and/or nuclei. Quartz is commonly incorporated in all samples and the range of variation is considerably small by up to a factor of two or three. The quartz contents appear to vary concordantly with nodule type and mineral composition. Nodule samples enriched in 10 Å manganate are also enriched in quartz, which may suggest dominant incorporation of detrital small particles of quartz from associated surface sediments into r-type nodules.

Phyllipsite is most abundant inside s-type nodules. It is attributable to frequent occurrence of zeolitic claystone served as nodule nuclei.

**Variability of internal structure of nodules on detailed survey lines**

Internal structure of nodules were described by means of megascopic and microscopic observations. Nodules consists principally of two ferromanganese constituents, with accessory manganese-free clayey silicate materials and nuclei.

Some workers proposed stratigraphic description of manganese nodules according to internal microstructure (SOREM and FOSTER, 1972; HEYE, 1975). I here proposed more definite criteria for nodule stratigraphy on the basis of mineralogy, which is more useful to description of internal structure of nodules and correlation between nodules. Two principal mineral phases, which exclusively consist representative microstructure, could be employed as stratigraphic units of nodules. Three units of ferromanganese materials are defined under reflecting microscope according to optical properties as follows:

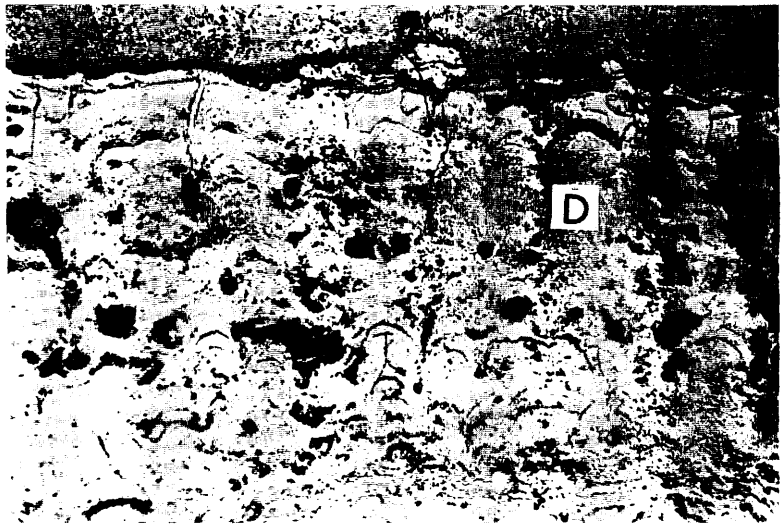


(A)

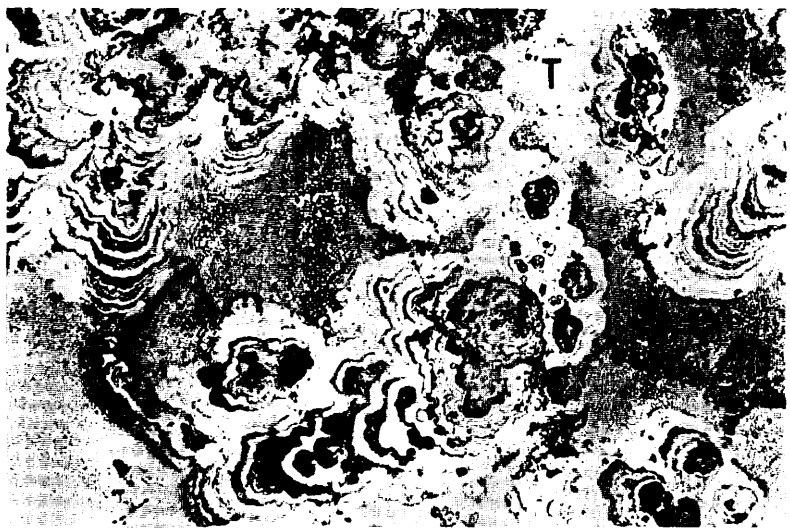


(B)

Fig. XIV–1 Photomicrographs of typical stratigraphic units of manganese nodules. A) δ–$MnO_2$ phase of stratified structure consisting smooth surface (D in photo), B) 10 Å manganate phase of cuspate or dendritic structure consisting rough surface (T in photo).

1) 10 Å manganate phase: cuspate or dendritic growth structure composing rough surface of nodules (Fig. XIV–1a),

2) δ–$MnO_2$ phase: monotonously stratified or massive structure composing smooth surface of nodules (Fig. XIV–1b),

3) fine alternations of the above two phases sometimes showing intermediate

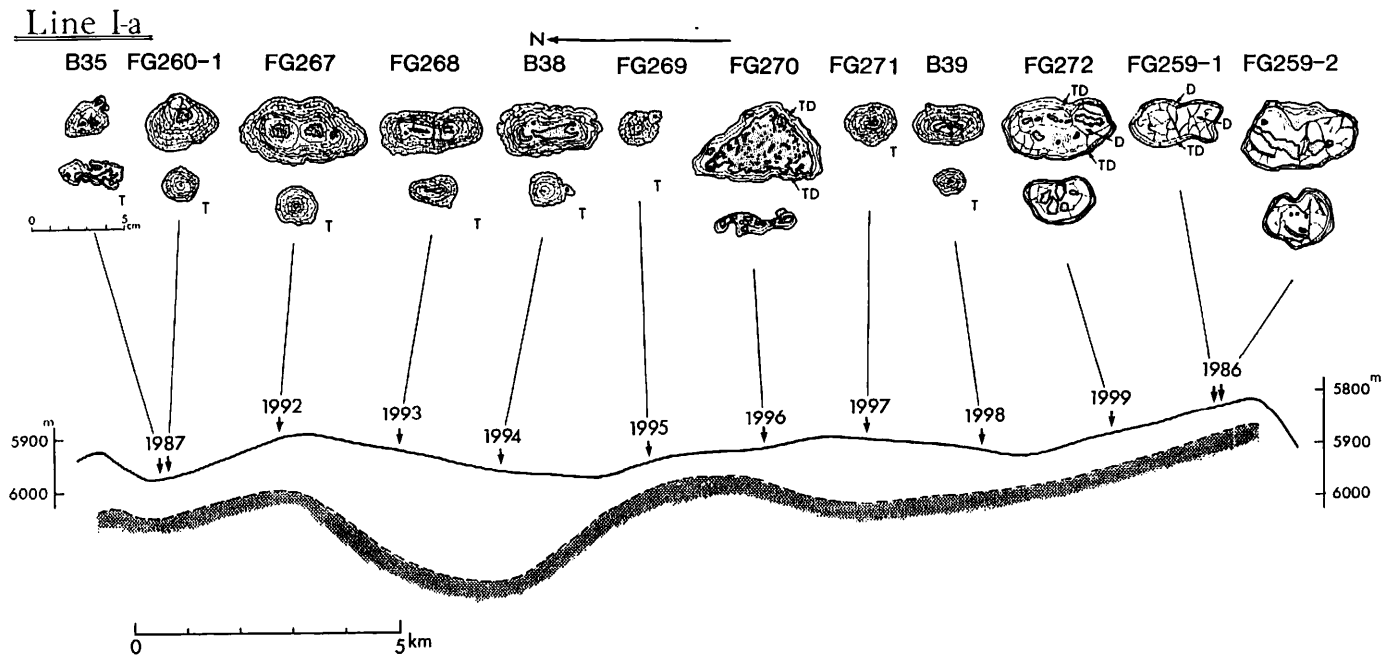


Fig. XIV-2 (1)

Fig. XIV–2 Variation of internal structure of manganese nodule on detailed survey lines. Shadows in topographic profiles denote opaque layers overlain by transparent layers in 3.5 kHz subbottom profiler. T, TD, DT, D denote manganese mineral abundance in this order.

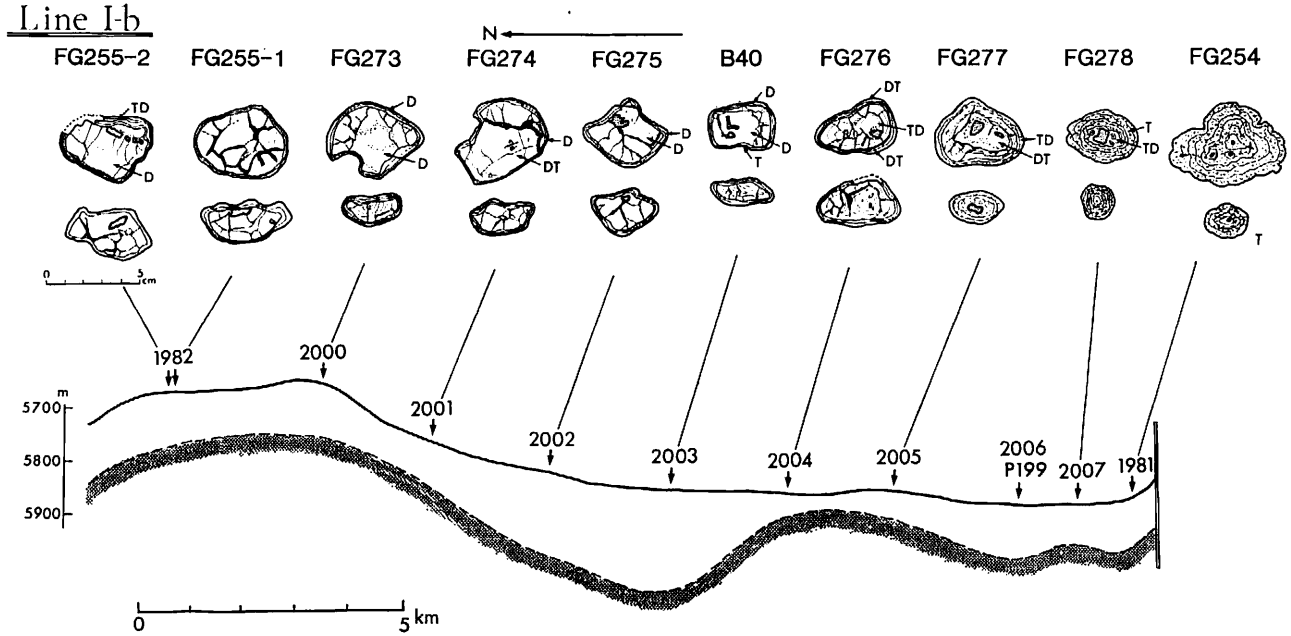
Line I-b
N
FG255-2
FG255-1
FG273
FG274
FG275
B40
FG276
FG277
FG278
FG254
TD
D
DT
T
0
5cm
1982
2000
2001
2002
2003
2004
2005
2006
P199
2007
1981
m
5700
5800
5900
0
5 km

Fig. XIV-2 (2)

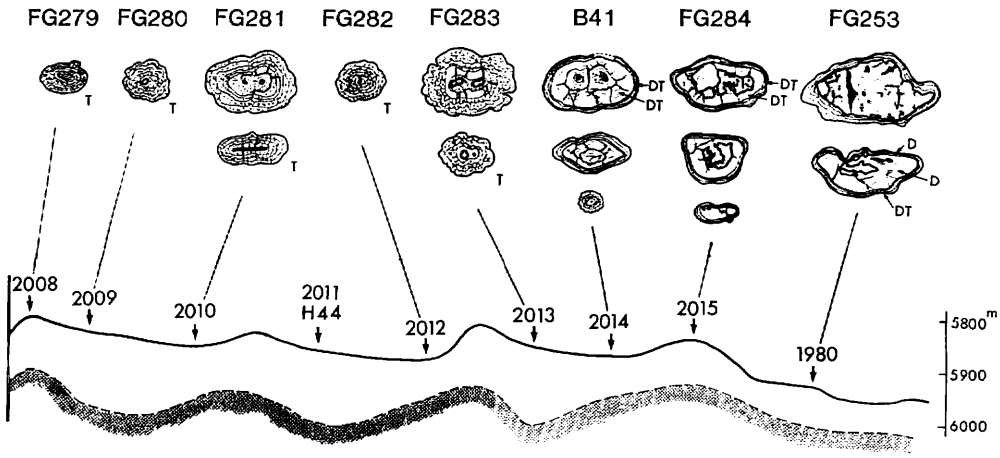


Fig. XIV-2 (3)

features as nodule surface, and another unit is nuclei composed of manganese-free material.

Megascopic description of polished nodule sections and related X-ray diffraction results are demonstrated in Figure XIV–2. Figure XIV–3 shows schematic stratigraphy of nodules along the surveyed lines.

The nodules frequently include conformable and unconformable boundaries between two phases. The unconformable boundary is characterized by sequential development of one unit of surrounding layer over the fragments of inside older nodules. This unconformable boundary is most dominant in smooth surface nodules of irregular shape. Internal older nodules often fragmented or fractured are composed of δ–$MnO_2$, while surrounding layers variable.

Along the detailed survey lines, nodule surface varies gradually or drastically from characteristic s-type to r-type nodules. However, the pattern of variation of internal structure is not always consistent with that of surface feature. On lines I–a and I–b the variation from types s to r are consistent with that of nodule internal structure. Type r is almost entirely composed of 10 Å manganate showing wholly concentric lamination, and type s is characterized by internal s-type nodules composed of δ–$MnO_2$ phase and structure composing rough surface of nodules (Fig. XIV–1a). On the other hand, on lines II–a, II–b and II–c, above mentioned relationship is not the case. Type r sometimes contains older s-type nodules comprising large-size nodules near the transitional zones from smooth to rough nodules, e. g., Sts. 2033, 2036 etc.

Therefore the areas distribution of outer 10 Å manganate phase and that of internal s-type nodules are not always exclusive to each other but in some cases the former overlap the latter in the Area II nodules. As shown in Figure XIV–2, The variability of internal structure has no distinct relationship to the topography or subbottom structure on 3.5 kHz SBP records. Only possible relationships are the dominant development of the 10 Å manganate phase on nodules from deeper basin areas of flat topography and that of the δ–$MnO_2$ phase inside nodules from topographic highs.

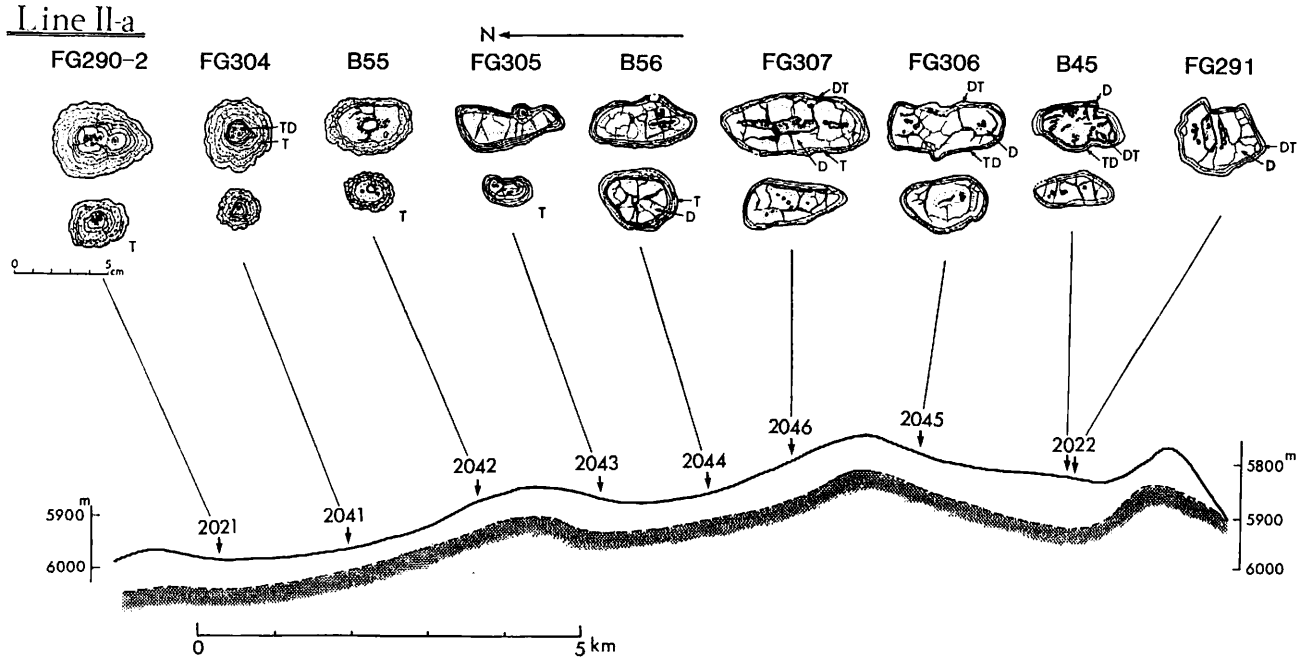
Line II-a
N
FG290-2
FG304
B55
FG305
B56
FG307
FG306
B45
FG291
TD
T
DT
D
0
5cm
2021
2041
2042
2043
2044
2046
2045
2022
5900m
6000
5800m
0
5km

Fig. XIV-2 (4)

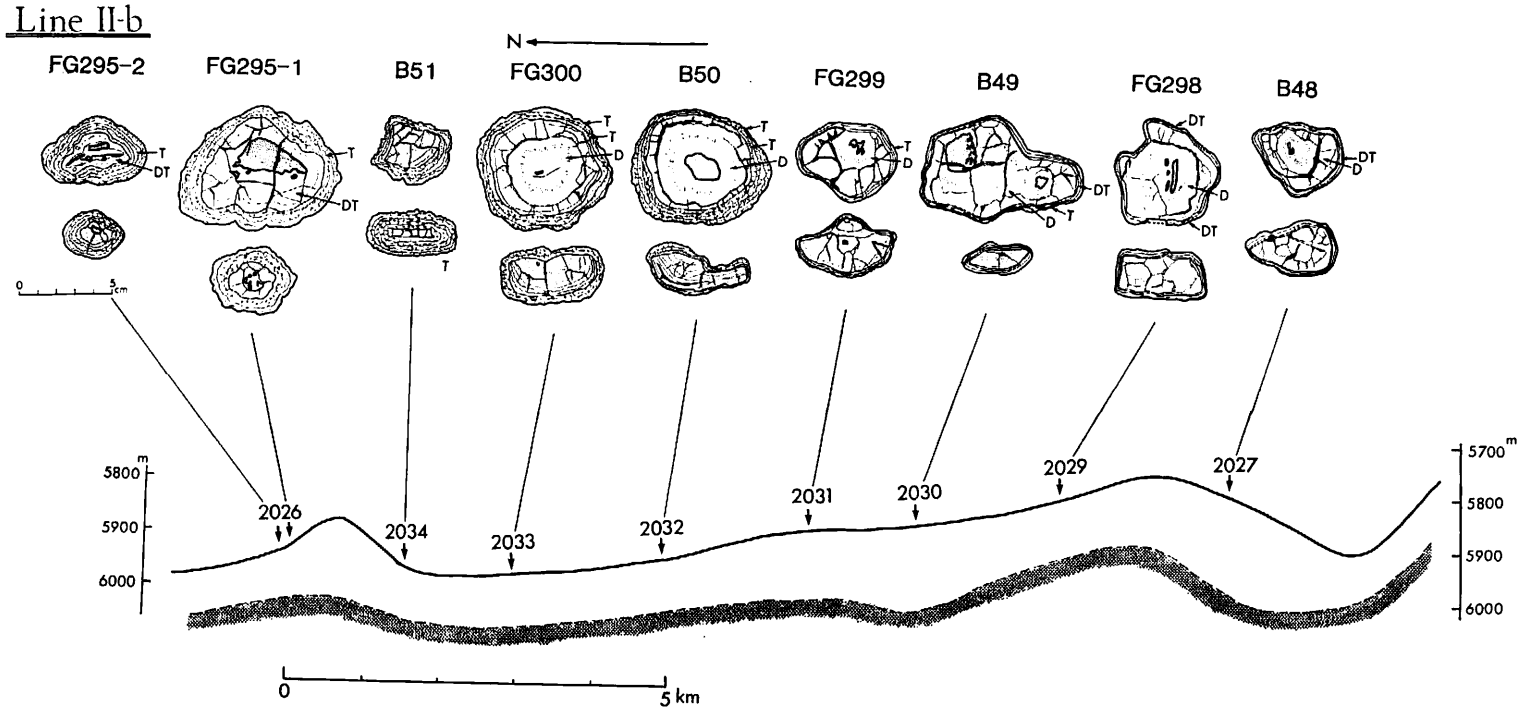
Line II-b
N
FG295-2
FG295-1
B51
FG300
B50
FG299
B49
FG298
B48
T
DT
D
0
5cm
5800m
5900
6000
2026
2034
2033
2032
2031
2030
2029
2027
5700m
5800
5900
6000
0
5 km

Fig. XIV-2 (5)

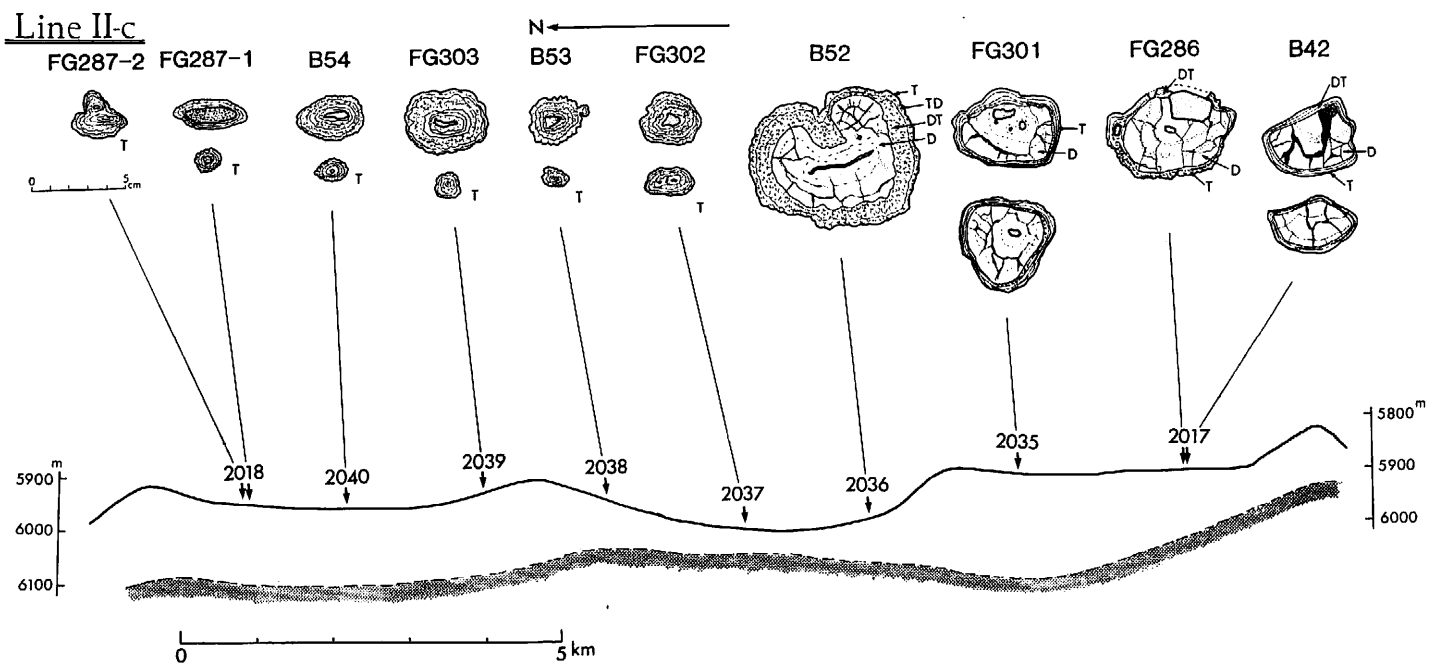
Line II-c
N
FG287-2
FG287-1
B54
FG303
B53
FG302
B52
FG301
FG286
B42
T
TD
DT
D
0
5cm
2018
2040
2039
2038
2037
2036
2035
2017
5900m
6000
6100
5800m
5900
6000
0
5 km

Fig. XIV-2 (6)

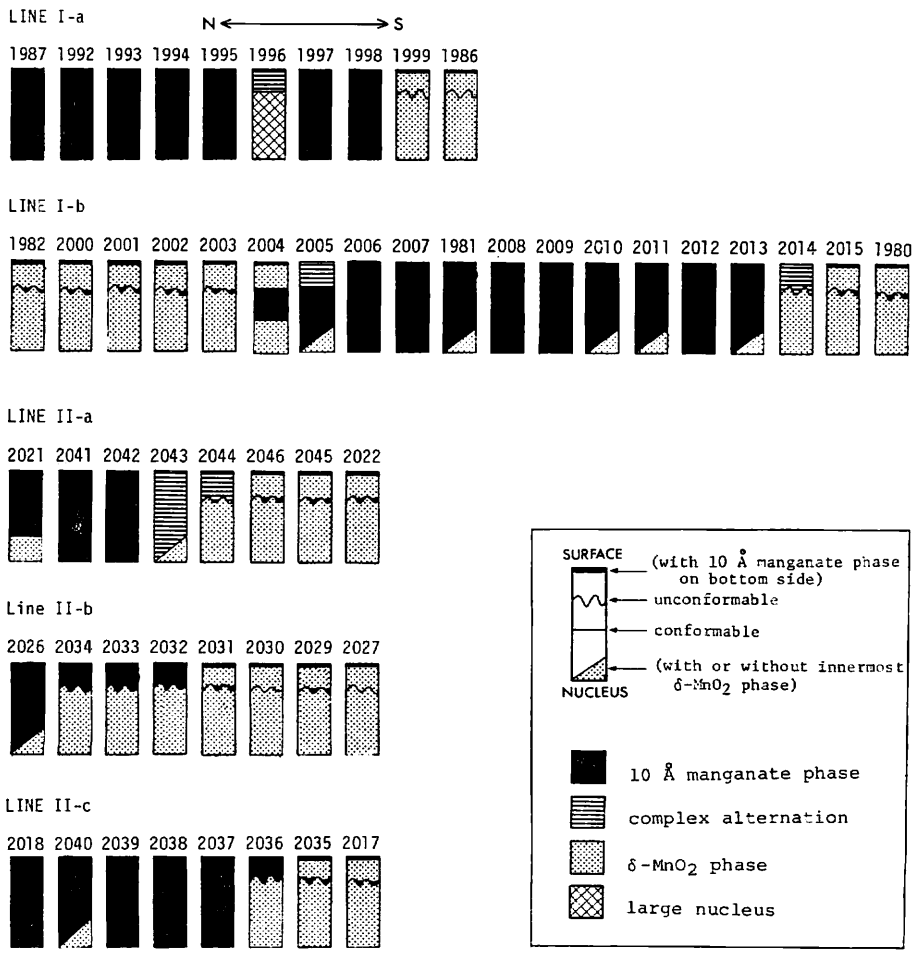


Fig. XIV–3 Schematic stratigraphy of manganese nodules interpreted by megascopic and microscopic observation of polished nodule sections and X-ray powder diffraction analyses.

Finely laminated unit (3) is dominantly observed on the nodule surface in the transitional zones from smooth to rough nodules, e. g., Sts. 1996, 2005, 2044 etc.

The older s-type nodule fragments in various nodules are significantly similar in microstructure and chemical composition (USUI and MOCHIZUKI, this cruise report) throughout the survey lines. The microstructure and chemical compositions of rough to intermediate surfaces composed of the 10 Å manganate are also fairly invariable despite morphological variability of nodules. This suggests a possibility of stratigraphic correlations of each phases between nodule samples. Schematic stratigraphy of manganese nodules reveals that deposition of the $\delta$–$MnO_2$ is clearly divided into two facies; one is as internal older nodules occasionally broken and the other is outermost surrounding layers of s-type nodules. The former developed lower the unconformable boundary is dominantly fractured and fragmented while the latter developed over the

boundary is of less fractures. It is also revealed that the internal s-type nodules appear to be deposited in the older age than the surrounding layers of 10 Å manganate and typical type r entirely composed of 10 Å manganate.

To sum up, manganese nodules of this area are initiated with dominant and extensive deposition of the $\delta$–$MnO_2$ and zeolitic claystones, followed by the fragmentation of these nodules. After the fragmentation, deposition of $\delta$–$MnO_2$ and 10 Å manganate took place on the fragmented nodules or another nuclei. Considering that both phases are interbedded in nodules around the transitional zones from type s to r, the deposition of the two phases appear to be simultaneous. Difference of nodule surfaces related to mineral composition is probably due to local difference in sedimentary conditions.

## References


ARRHENIUS, G., CHEONG, K., CRANE, S., FISK, M., FRAZER, J., KORKISCH, J., MELLIN, T., NAKAO, S., TSAI, S. and WOLF, G. (1979) Counterions in marine manganate. *In* C. Lalou (ed.) *La genése des Nodules de Manganése*, Colloques. Intern. du CNRS, no. 289, p. 333–356.

BURNS, R. G. and BURNS, V. M. (1977) Mineralogy of manganese nodules. *In* G. P. Glasby (ed.) *Marine Manganese Deposits*, Elsevier, New York, p. 185–248.

BURNS, R. G. and BURNS, V. M. (1979) Manganese oxides. *In* R. G. Burns (ed.) *Marine Minerals*, Mineral. Soc. America Short Course Notes, vol. 6., p. 1–46.

BUSER, W. and GRÜTTER, A. (1956) Über die Natur der Manganknollen. *Scweiz. Min. Petr. Mitt.*, vol. 36, p. 49–62.

CHUKHROV, F. V., GORSHKOV, A. I., SIVTSOV, A. V. and BEREZOVSKAYA, V. V. (1979) A new 14 Å mineral of the birnessite group in deep-sea micronodules. *Nature*, vol. 28, p. 136–137.

GIOVANOLI, R. and BÜRKI, P. (1975) Comparison of X-ray evidence of marine manganese nodules and non-marine manganese ore deposits. *Chimia*, vol. 29, p. 266–269.

HEYE, D. (1975) Wachstumsverhältnisse von Manganknollen. *Geol. Jahrbuch*, Reihe E., Heft 5, pp. 1–122.

SOREM R. K. and FOSTER A. R. (1972) Internal structure of manganese nodules and implications in benefication. *In* D. R. Horn (ed.) *Ferromanganese Deposits on the Ocean Floor*, p. 167–182.

USUI, A. (1979) Minerals, metal contents, and mechanism of formation of manganese nodules from the Central Pacific Basin (GH76–1 and GH77–1 areas). *In* J. L. Bischoff and D. Z. Piper (eds.) *Marine Geology and Oceanography of the Pacific Manganese Nodule Province*. Marine Science Ser. 9., Plenum Publ. Corp., New York, p. 651–679.

USUI, A. (1982) Variability of manganese nodule deposits: the Wake-Tahiti Transect. *Geol. Surv. Japan Cruise Rept.*, no. 18, p. 138–224.